Sensors and Actuators B 195 (2014) 1–7

Contents lists available at ScienceDirect

Sensors and Actuators B: Chemical

journal homepage: www.elsevier.com/locate/snb

Dendritic copper-cobalt nanostructures/reduced graphene oxide-chitosan modified glassy carbon electrode for glucose sensing

Li Wang[a], Yaolin Zheng[a], Xingping Lu[a], Zhuang Li[b], Lanlan Sun[c], Yonghai Song[a,*]

[a] Key Laboratory of Chemical Biology, Jiangxi Province, Key Laboratory of Functional Small Organic Molecule, Ministry of Education, College of Chemistry and Chemical Engineering, Jiangxi Normal University, Nanchang 330022, China
[b] State Key Laboratory of Electroanalytical Chemistry, Changchun Institute of Applied Chemistry, Chinese Academy of Sciences, Changchun, 130022 Jilin, China
[c] State Key Laboratory of Luminescence and Applications, Changchun Institute of Optics, Fine Mechanics and Physics, Chinese Academy of Sciences, 3888 East Nan-Hu Road, Changchun 130033, China

ARTICLE INFO

Article history:
Received 4 September 2013
Received in revised form
25 November 2013
Accepted 3 January 2014
Available online 10 January 2014

Keywords:
Cu-Co nanostructures
Reduced graphene oxide
Chitosan
Electrocatalysis
Glucose
Sensor

ABSTRACT

A novel nonenzymatic glucose sensor was developed by electrodepositing dendritic copper-cobalt nanostructures (Cu-Co NSs) on glassy carbon electrode (GCE) which was modified by reduced grapheme oxide-chitosan (RGO-CHIT) nanocomposites. The electrochemical behaviors and electrocatalytic performances of the sensor towards oxidation of glucose were evaluated by cyclic voltammograms, chronoamperometry and amperometric method. Compared to sensors based on monometal Cu or Co NSs, the sensor based on bimetal Cu-Co NSs exhibits good electrocatalytic activity towards oxidation of glucose. The effects of electrodeposition time and the ratio of Cu^{2+} and Co^{2+} in an electrodeposition solution on the electrocatalytic performance of the Cu-Co NSs sensor were explored in detail. The best catalytic activity towards oxidation of glucose can be achieved under an optimized condition: electrodepositing time of 2600 s and the Cu^{2+}/Co^{2+} molar ratio of 2:1. The catalytic current density is linear to the glucose concentration in the range of 0.015–6.95 mM ($r = 0.9947$) with a sensitivity of 1921 $\mu A\,cm^{-2}\,mM^{-1}$, and a detection limit of 10 μM. The good catalytic activity, high sensitivity and good stability indicate that the newly developed sensor based on the dendritic Cu-Co NSs/RGO-CHIT/GCE is a promising sensor for application in real samples.

1. Introduction

Glucose is one of the essential substances for life activities, and it can provide energy to maintain the normal life activities by ingesting directly in the metabolic process. Glucose is widely distributed in blood of being livings [1], and the concentration increase of glucose in blood could cause diabetes mellitus. The diabetes mellitus has become one of the major health afflictions worldwide [2]. Therefore, quantitative determination of glucose concentration both in blood and in other sources such as foods and pharmaceuticals is very important in biological and clinical analysis [3,4].

Graphene or reduced graphene oxide (RGO), the thinnest two-dimensional carbon material, can provide a good supporting for metal nanomaterials deposition or enzyme adsorption on electrodes because of its large theoretical specific surface area ($2630\,m^2\,g^{-1}$) [5,6]. The large specific surface area, high electrical conductivity and wide electrochemical window have led it to be one of the most important materials in electrochemical sensors [7,8]. Chitosan (CHIT) possesses distinct chemical and biological properties owing to the existence of many reactive amino and hydroxyl groups. It is considered to be a promising material for modification of the electrode surface as well as a very good matrix for nanomaterials and enzyme immobilization due to its good stability, a large number of functional groups, high permeability toward water and excellent film-forming ability [9–11]. Therefore, the CHIT has been chosen as reduction and functionalized agent to reduce and functionalize graphene oxide (GO) for preparing RGO-CHIT, which exhibits many good properties over CHIT or RGO as electrode materials for preparing glucose sensor.

Metal or metal oxide nanostructures (NSs) modified electrodes as nonenzymatic glucose sensors have raised particular interest [12–14]. Many metal or metal oxide NSs, including Au NSs [15,16], Cu_2O NSs [17], Cu NSs[18,19], CoO NSs [20], Co NSs [21] etc, have been used to modify the electrodes for glucose detection, especially bimetal NSs. The multiple functionalities, good selectivity, remarkable catalytic activity, and high stability over monometal NSs have led the bimetal NSs to be an ideal material in electrochemical sensors [22–29]. For example, Au-Ag NSs [22], Pt-Ni NSs [25],

* Corresponding author. Tel.: +86 791 88120862; fax: +86 791 88120862.
E-mail addresses: yhsonggroup@hotmail.com, yhsong@jxnu.edu.cn (Y. Song).

0925-4005/$ – see front matter © 2014 Elsevier B.V. All rights reserved.
http://dx.doi.org/10.1016/j.snb.2014.01.007

Pt-Co NSs [26] and Ni-Cu NSs [27] exhibit better catalytic activities and high sensitivity for glucose detection than their corresponding monometallic counterparts due to the synergistic effect of two metals. The previous results indicate that the design and fabrication of bimetal NSs with three-dimensional (3D) porous structure modified electrode is effective in achieving high sensitivity and low applied potentials for glucose detection.

Cu NSs and Co NSs have attracted extensive attention as economical electrocatalysts for nonenzymatic glucose sensors and amino acid sensors [18,30–32]. In this work, a facile strategy was used to prepare the dendritic Cu-Co NSs/RGO-CHIT/glassy carbon electrode (GCE) by electrodepositing the dendritic Cu-Co NSs on RGO-CHIT/GCE as a sensitive nonenzymatic glucose sensor. The Cu-Co NSs/RGO-CHIT/GCE exhibits large specific surface area and high catalytic activity towards the oxidation of glucose. The electrochemical properties and electrocatalytic activity of the sensor have been investigated in detail. The analytical parameters (such as linear range, detection limit and sensitivity) and the kinetic parameters (such as the diffusion coefficient and the catalytic rate constant) of the Cu-Co NSs/RGO-CHIT/GCE were both explored.

2. Experimental

2.1. Chemicals and reagents

CHIT was obtained from the Sigma–Aldrich (Milwaukee Wisconsin). Graphite powder, $CoCl_2{\cdot}6H_2O$ and $CuCl_2$ were purchased from Sinopharm Chemical Reagent Co., LTD (Tianjin, China). Na_2SO_4 and NaOH were purchased from Tianjin Fuchen Chemical Reagent Factory (Tianjin, China). Fetal calf serum was purchased from Thermo Fisher Scientific (Beijing, China). Other reagents were purchased from Beijing Chemical Reagent Factory (Beijing, China). All reagents were of analytical grade and used without further purification. All solutions were prepared with ultra-pure water, purified by a Millipore-Q system (18.2 MΩ cm).

2.2. Synthesis of graphene oxide (GO) and RGO-CHIT

The GO was synthesized according to Hummers' method [33]. The RGO-CHIT nanocomposites were prepared as follows [34]. 10.0 mg RGO was dissolved in 10.0 mL of ultra-pure water and ultrasonicated for 45 min. 10.0 mL CHIT solution (1.0 wt.%) was prepared by dissolving CHIT in 0.5 vol.% aqueous acetic acid solution. Then RGO solution was added into the CHIT solution and stirred for 24 h to produce the RGO-CHIT dispersion.

2.3. Preparation of the Cu-Co NSs/RGO-CHIT/GCE

10 μL RGO-CHIT dispersion was cast onto the polished GCE, and dried for 10 h in air to obtain the RGO-CHIT/GCE. Then the Cu-Co NSs/RGO-CHIT/GCE was prepared by electrodepositing in a 0.1 M Na_2SO_4 + 0.01 M $CuCl_2$ + 0.01 M $CoCl_2$ solution at −0.95 V. The mixed solution was purged with nitrogen gas for 30 min before the electrodepositing. For comparison, the Cu NSs/RGO-CHIT/GCE and the Co NSs/RGO-CHIT/GCE were also prepared with the same procedure as described above.

2.4. Instrumentations

All electrochemical experiments were performed on a CHI760d electrochemical workstation (CH Instruments, Shanghai, China) using a conventional three-electrode system with a platinum wire as the auxiliary electrode, a bare or modified GCE as the working electrode, and a saturated calomel electrode (SCE) as the reference electrode. The cyclic voltammetric experiments were performed in a quiescent solution. The amperometric were carried out in a beaker with continuous stirring using a magnetic stirrer. Scanning electron microscopy (SEM) analysis was taken using a XL30 ESEM-FEG SEM at an accelerating voltage of 20 kV equipped with a Phoenix energy dispersive X-ray analyzer.

3. Results and discussion

3.1. Electrodeposition of Cu-Co NSs on RGO-CHIT/GCE

Cyclic voltammograms (CVs) was utilized to monitor the electrodeposition process of Cu-Co NSs on RGO-CHIT/GCE. As shown in Fig. 1, there were three cathodic peaks and three anodic peaks. The cathodic peak at −0.86 V (peak I′) was attributed to the reduction of Co^{2+} on the electrode surface to form Co NSs, and the corresponding anodic peak I might be due to the dissolution of the Co NSs [35]. The cathodic peak at −0.26 V (peak II′) and −0.06 V (peak III′) were related to the reduction of Cu^{2+} to Cu^{+} and Cu^{+} to Cu NSs, respectively [36]. The corresponding anodic peaks II and III might be due to the two-step oxidation of the Cu NSs. The result indicated that Cu^{2+} and Co^{2+} could be reduced to Cu-Co NSs at −0.95 V. With the increasing of potential scan number, the Cu-Co NSs grew on the electrode surface because the oxidation peak increased and the reduction peak decreased gradually.

The formation of Cu-Co NSs/RGO-CHIT/GCE at different electrodepositing time was characterized by CVs in 0.1 M NaOH. As shown in Fig. 2A, the peak current density increased gradually with the increase of electrodeposition time from 600 s to 2600 s. After the electrodeposition time exceeded 2600 s, the peak current density decreased and the shape of peaks changed. The plot of peak current density versus electrodepositing time exhibited a turning point at about 2600 s (inset in Fig. 2A). The turning point might be ascribed to the fact that the Cu-Co NSs became rather large with excessive electrodeposition time, and finally resulted in the decrease of electrochemical activity.

The electrochemical behaviors of Cu-Co NSs/RGO-CHIT/GCE were investigated by CVs at different scan rates in 0.1 M NaOH solution (Fig. 2B). Obviously, the peak current density was enhanced with the increasing of scan rate. It was noticeable that another pairs of redox peaks appeared at about 0.4 V for anodic peak and 0.1 V for cathodic peak at high scan rate. According to the previous conclusion, the three pairs of redox peaks might be assumed as follows [37–40]:

$$Cu(0) + 2OH^- \leftrightarrow Cu(OH)_2 + 2e \quad (1)$$

$$Co(0) + 2OH^- \leftrightarrow Co(OH)_2 + 2e \quad (2)$$

$$\text{Peak } a_1/c_1\text{: } Co(OH)_2 + OH^- \leftrightarrow CoOOH + H_2O + e \quad (3)$$

$$\text{Peak } a_2/c_2\text{: } CoOOH + OH^- \leftrightarrow CoO_2 + H_2O + e \quad (4)$$

$$\text{Peak } a_3/c_3\text{: } Cu(OH)_2 + OH^- \leftrightarrow CuOOH + H_2O + e \quad (5)$$

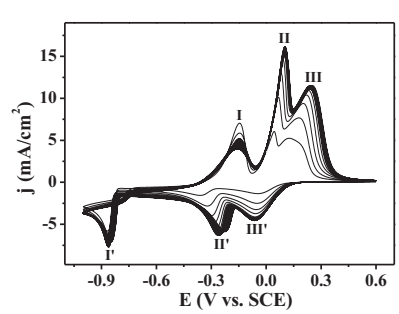

Fig. 1. CVs of RGO-CHIT/GCE in 0.1 M Na_2SO_4 + 0.01 M $CuCl_2$ + 0.01 M $CoCl_2$ at 50 mV s^{-1}.

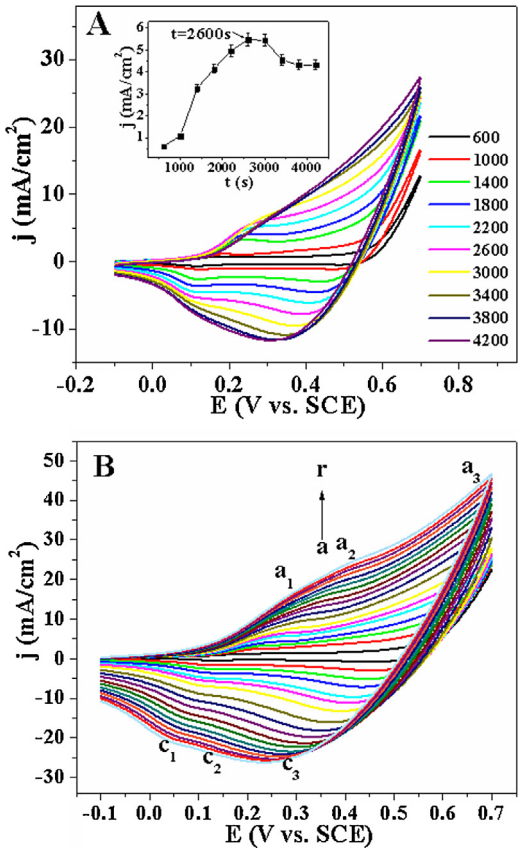

Fig. 2. (A) CVs of Cu-Co NSs/RGO-CHIT/GCE obtained at various electrodeposition times in 0.1 M NaOH at 50 mV s^{-1}. Inset: plot of peak current density at 0.24 V vs. electrodeposition time. (B) CVs of Cu-Co NSs/RGO-CHIT/GCE in 0.1 M NaOH at different scan rates: 10 (a), 30 (b), 50 (c), 70 (d), 100 (e), 120 (f), 150 (g), 200 (h), 250 (i), 300 (j), 350 (k), 400 (l), 450 (m), 500 (n), 550 (o), 600 (p), 650 (q) and 700 (r) mV s^{-1}.

First, the Co (0) and Cu (0) was transformed into $Co(OH)_2$ and $Cu(OH)_2$ in the alkaline conditions, and then further oxidized into CoO_2 and CuOOH as potential shifted to the positive direction. The CoO_2 and CuOOH can be used as heterogeneous catalysts with good chemical stability and electrocatalytic activity [40,41].

3.2. Characteristics of the as-prepared Cu-Co NSs/RGO-CHIT/GCE

Fig. 3 revealed the SEM images of Cu NSs/RGO-CHIT/GCE, Co NSs/RGO-CHIT/GCE, Cu-Co NSs/RGO-CHIT/GCE and Cu-Co NSs/GCE. As can be seen in Fig. 3A, the Cu NSs on RGO-CHIT/GCE was amorphous and irregular. The doping of Co resulted in the formation of 3D porous dendrites (Fig. 3B). The image of the elements in the inset of Fig. 3B showed that the Cu (green) and Co (red) were uniformly distributed on the surface of the electrode. While only a few leaf-like Co nanosheets and a large amount of flower-like Co NSs were formed on the RGO-CHIT/GCE surface (Fig. 2C). It indicated clearly that the doping of Co played a key role in the evolution of 3D dendritic Cu-Co NSs. It was possible that the nucleation of Cu-Co NSs might be accelerated in the coexistence of bimetal and accordingly resulted in the formation of many 3D porous dendrites [42–44]. The Cu might accelerate the growth of sub-branches [42], and the Co might be benefit to the formation of the dendrites [45]. Energy dispersive X-ray spectroscopy (EDX) was used to study the components of the Cu-Co NSs/RGO-CHIT/GCE (Fig. 3D) and it clearly indicated that the Cu-Co NSs/RGO-CHIT/GCE mainly contained Cu and Co elements. The inserted table in Fig. 3D demonstrated that the molar ratio of the two components was slightly larger than that of initial precursor solution [46].

It was noticeable that a lot flower-like spherical and few dendrites nanostructures were found on Cu-Co NSs/GCE surface without RGO-CHIT (Fig. 3E). Obviously, the RGO-CHIT provided a large specific surface area with more binding-sites to increase the quantity of dendritic Cu-Co NSs. Fig. 3F–H showed SEM images of Cu-Co NSs obtained at Cu^{2+}/Co^{2+} ratio of 2:1 with the potential of −0.95 V under different deposition time. Fig. 3F showed a typical SEM image of the RGO-CHIT/GCE, and it indicated that the

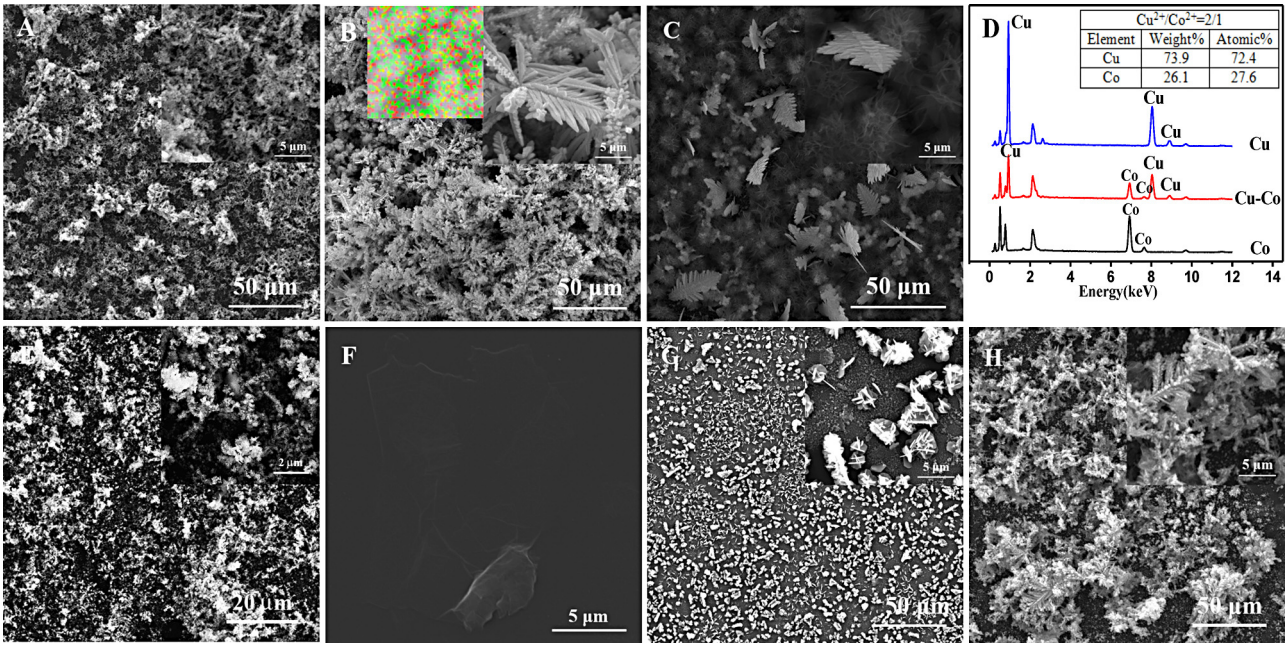

Fig. 3. SEM images of the Cu NSs/RGO-CHIT/GCE (A), Cu-Co NSs/RGO-CHIT/GCE (B) and Co NSs/RGO-CHIT/GCE (C). (D) Energy dispersive X-ray spectra of electrode. (E) SEM image of the Cu-Co NSs/GCE. SEM images of the Cu-Co NSs/RGO-CHIT/GCE at different electrodeposition time: 0 s (F), 100 s (G) and 600 s (H).

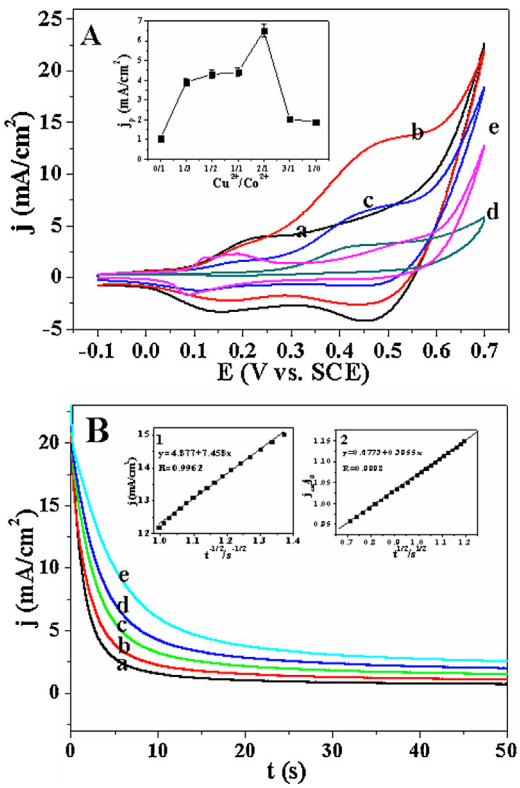

Fig. 4. (A) CVs of different electrodes in 0.1 M NaOH in absence (a) and presence of 1.0 mM glucose (b–e) at 50 mV s^{-1}: (a) Cu-Co NSs/RGO-CHIT/GCE, (b) Cu-Co NSs/RGO-CHIT/GCE, (c) Cu-Co NSs/GCE, (d) Cu NSs/RGO-CHIT/GCE and (e) Co NSs/RGO-CHIT/GCE. Inset: the plot of catalytic current density vs. the ratio of Cu^{2+} and Co^{2+}. (B) Chronoamperograms of Cu-Co NSs/RGO-CHIT/GCE in 0.1 M NaOH solution with different concentrations of glucose: 0 mM (a), 1.0 mM (b), 2.0 mM (c), 3.0 mM (d) and 4.0 mM (e). Applied potential was 420 mV. Inset 1: dependency of transient current density on $t^{-1/2}$. Inset 2: dependency of j_{cat}/j_d on $t^{1/2}$ derived from the data of chronoamperograms of curves a and e in panel (B).

RGO-CHIT surface was smooth and homogeneous. After electrodeposition for 100 s, a large number of flower-like Cu-Co NSs were synthesized on RGO-CHIT/GCE surface (Fig. 3G). As the deposition time was increased to 600 s (Fig. 3H), the nanoflowers provided a lot of node for the formation of dendirtic structure. With further prolonging the deposition time to 2600 s, the dendritic structure becomes more and more distinct (Fig. 3B). As we all known, the 3D dendirtic structure allows rapid transportation of the electrolytes and exhibits high specific surface area. Therefore, Cu-Co NSs with 3D dendirtic structures are promising materials for glucose sensors.

3.3. Electrocatalytic oxidation of glucose at Cu-Co NSs/RGO-CHIT/GCE

As shown by curve b in Fig. 4, after 1.0 mM glucose was added into the solution, the anodic peak current density related to the oxidation of $Cu(OH)_2$ and CoOOH species at 0.45 V were increased and the corresponding cathodic current density were decreased as compared to that in absence of glucose (curve a), which is typical catalytic reaction. Compared to the other electrodes (curve c, d and e), the Cu-Co NSs/RGO-CHIT/GCE (curve b) exhibited outstanding electrochemical performance with the highest peak current density and the lowest peak potential. The inset in Fig. 4A showed the plot of catalytic current density versus the molar ratio of Cu^{2+}/Co^{2+}. It clearly indicated that the 3D dendirtic Cu-Co NSs/RGO-CHIT/GCE exhibited the highest catalytic response when the ratio of Cu^{2+}/Co^{2+} was 2/1.

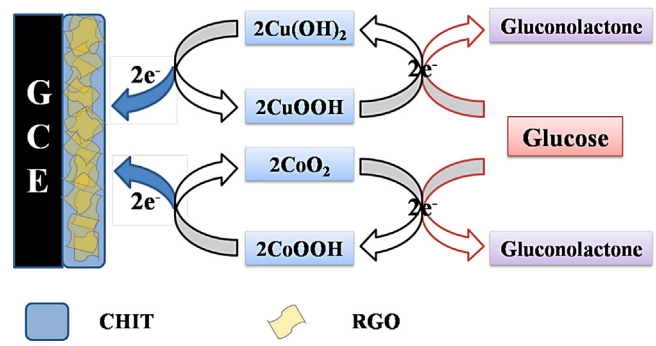

Fig. 5. Schematic illustration of glucose electrocatalytic reaction mechanism.

Fig. 4B showed the chronoamperometry response for Cu-Co NSs/RGO-CHIT/GCE in the absence (curve a) and presence (curve b–e: 1.0–4.0 mM) of glucose. After the applied potential was stepped to 420 mV, a large anodic current density occured because the glucose began to be oxidized. Then as the glucose near electrode surface was oxidized into gluconolactone, the catalytic current density decreased gradually. Finally, a stable concentration difference of glucose between electrode surface and bulk solution was obtained and the catalytic current density was maintained as shown by the curves (a–e) in Fig. 4B. The time when the catalytic current density decreased to stable value depends on the catalytic rate constants (K_{cat}) and accordingly the chronoamperograms could be used to calculate the K_{cat}. The relationship between the net current density and the minus square roots of time was shown in inset 1 (Fig. 4B), and it revealed a linear dependency. It demonstrated that the electrocatalytic oxidation of glucose was a diffusion-controlled process. The diffusion coefficient (D) of glucose could be estimated according to Cottrell equation [47]:

$$j = \frac{I}{A} = nFD^{1/2}C\pi^{-1/2}t^{-1/2} \quad (6)$$

where j is the current density, I is the current, A is the electrode surface geometrical area, n is the electron transfer number, F is the Faraday constant (F = 96493 C mol^{-1}), C is the bulk concentration and t is the elapsed time. The mean value of the diffusion coefficient of glucose was found to be 1.22×10^{-3} cm^2 s^{-1} by using the slope of the line in inset 1 (Fig. 4B). Chronoamperometry could also be used for the evaluation of the K_{cat} with the help of the following equation [48]:

$$\frac{j_{cat}}{j_d} = \pi^{1/2}(K_{cat}Ct)^{1/2} \quad (7)$$

where j_{cat} and j_d are the catalytic current density and the diffusion-controlled current density, respectively. From the slope of the j_{cat}/j_d vs. $t^{1/2}$ plot, as shown in inset 2 (Fig. 4B), the mean value of K_{cat} for glucose was obtained as 4.98×10^4 cm^3 mol^{-1} s^{-1}.

According to the above results and previous conclusion, the possible redox mechanism can be assumed as shown in Fig. 5. The catalytic mechanism for the glucose oxidation might be assumed as following. $Cu(OH)_2$ and CoOOH were firstly oxidized into CuOOH and CoO_2, respectively, and then the glucose was oxidized by CuOOH and CoO_2, which resulted in the regeneration $Cu(OH)_2$ and CoOOH [37–40,49,50].

3.4. Calibration curve

Amperometric measurements were carried out at 0.45 V at the Cu-Co NSs/RGO-CHIT/GCE by successive injection of glucose (curve 1 in Fig. 6A) into a stirring 0.1 M NaOH. The oxidation current density reached a maximum steady-state value and achieved 95% of the steady-state current density within 3 s. The curve 1

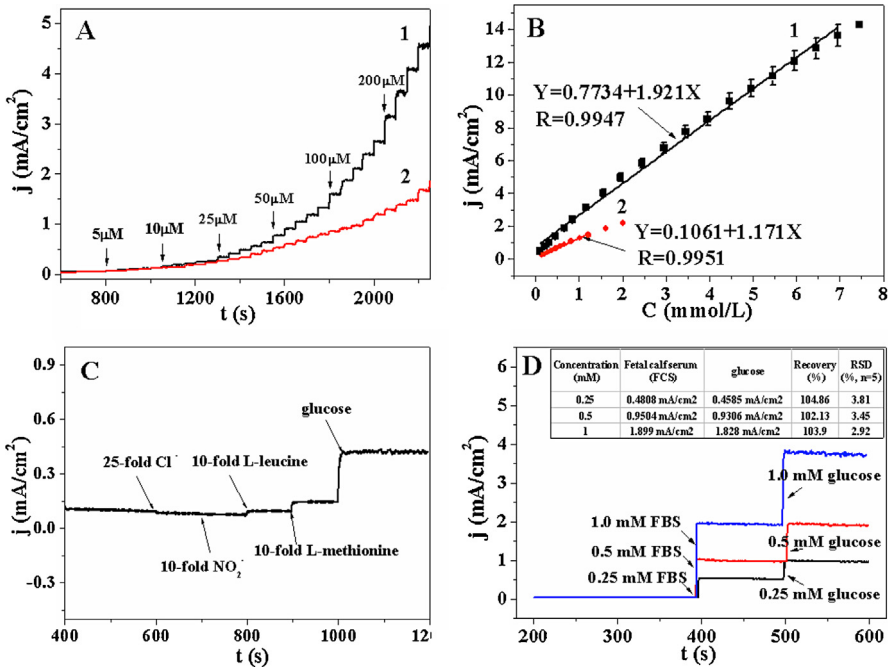

Concentration (mM)	Fetal calf serum (FCS)	glucose	Recovery (%)	RSD (%, n=5)
0.25	0.4808 mA/cm2	0.4585 mA/cm2	104.86	3.81
0.5	0.9504 mA/cm2	0.9306 mA/cm2	102.13	3.45
1	1.899 mA/cm2	1.828 mA/cm2	103.9	2.92

Fig. 6. (A) Typical steady-state response of Cu-Co NSs/RGO-CHIT/GCE (1) and Cu-Co NSs/GCE (2) to successive injection of glucose into the stirring 0.1 M NaOH. (B) The plot of the calibration curve. (C) Chronoamperometric responses for glucose and interference of Cl^-, NO_2^-, L-leucine and L-methionine. (D) Detection of simulative practical samples. Applied potential: 0.45 V and supporting electrolyte: 0.1 M NaOH.

in Fig. 6B showed the calibration curve of the sensor. The linear range of the glucose detection was from 0.015 mM to 6.95 mM (r = 0.9947) with a slope of 1921 $\mu A\,cm^{-2}\,mM^{-1}$, and a detection limit of 10 μM (S/N = 3). For comparison, the amperometric response of the Cu-Co NSs/GCE towards the oxidation of glucose (curve 2 in Fig. 6A) was investigated. The linear range of the glucose detection was from 0.015 mM to 1.21 mM (r = 0.9947) with a slope of 1171 $\mu A\,cm^{-2}\,mM^{-1}$, and a detection limit of 10 μM (S/N = 3) (curve 2 in Fig. 6B). It indicated clearly that Cu-Co NSs/RGO-CHIT/GCE possessed a better catalytic activity and sensitivity towards the oxidation of glucose.

Interference is inevitable in the determination of some analytes, and thus interference of some chemicals was investigated in this work as shown in Fig. 6C. Chemicals such as Cl^- in a 25-fold, NO_2^-, L-leucine and L-methionine in a 10-fold concentration did not show obvious interference to glucose detection, indicating the good selectivity. The stability of the sensor was also investigated. After the sensor was stored in the inverted beaker at atmosphere for 30 days, the current response to 1.0 mM glucose was decreased by 3.6% of the original current. The repeatability of the current signal of the same electrode for 1.0 mM glucose was examined in 0.1 M NaOH. The relative standard deviation (RSD) was 2.0% for six successive measurements. The electrode-to-electrode repeatability was determined from the response to 1.0 mM glucose at five different sensors, and a RSD of 7.2% was achieved.

The further detection of glucose under coexistence of fetal calf serum (FCS) was performed on Cu-Co NSs/RGO-CHIT/GCE by amperometric measurements at 0.45 V. In brief, the same concentration (0.25, 0.5, 1.0 mM) of FCS samples and glucose were successive injection into a stirring 0.1 M NaOH (Fig. 6D). The results demonstrated good accuracy for the real samples. As shown by the inset table of Fig. 6D, the recoveries of glucose detection were between 102% and 105%. The RSD was obtained under 5 successive detections. The results revealed that the practical samples have a slightly high response current density than glucose, which might be ascribed to the amino acid found in the FCS. The result indicates that this sensor is effective in practical applications.

Up to now, many sensors have been developed for the detection of glucose based on Cu or Co nanomaterials, and all of them have some advantages and limitations. A comparison of the performance

Table 1
Comparison of various non-enzymatic glucose sensors.

Electrode	Detection potential (V)	Sensitivity ($\mu A\,cm^{-2}\,mM^{-1}$)	Linear range (mM)	Detection limit (mmol L^{-1})	Year	References
Cu-CoNSs/CHIT-RGO	0.45 (vs. SCE)	1921	0.015–6.95	0.01	-	This work
Cu-CoNSs	0.45 (vs. SCE)	1171	0015–1.21	0.01	-	This work
Cu NPs/grapheme	0.5 (vs. SCE)	-	Up to 4.5	0.0005	2012	[30]
Cu nanocubes/MWCNTs[a]	0.55 (vs. Ag/AgCl)	1096	Up to 7.5	0.001	2010	[51]
Cu nanowires/GTE[b]	0.6 (vs. SCE)	1100	0.005–6.0	0.0016	2013	[52]
Cu nanowires–MWCNTs	0.55 (vs. Ag/AgCl)	1995	Up to 3	0.005	2013	[18]
CoO nanorods	0.5 (vs. Ag/AgCl)	571.8	Up to 3.5	0.000058	2011	[20]
$CoO_x \cdot nH_2O$ MWCNTs	0.55 (vs. Ag/AgCl)	162.8	Up to 4.5	0.002	2011	[53]
Ni-Co NSs/RGO	0.5 (vs. SCE)	1773.6	0.01–2.65	0.00379	2013	[54]
Pt-Co alloy	0.6 (vs. SCE)	-	0.05–3.0	0.0001	2013	[55]
Ni–Cu/TiO_2 NTs[c]	0.6 (vs. Ag/AgCl)	1590.9	0.010–3.2	0.005	2013	[56]

[a] Multi-wall carbon nanotuber.
[b] Graphene transparent electrode.
[c] Nanotube arrays.

of our newly designed sensor with those already reported in literature regarding the performance of the glucose assay was shown in Table 1. By comparing, it could be clearly seen that the Cu-Co NSs/RGO-CHIT/GCE offered a reasonable linear range and detection limit, but the sensitivity was highest and the applied potential was lowest among these sensors. As shown in Fig. 3, the incorporation of Co resulted in the formation of 3D dendritic Cu-Co NSs. The porous dendritic Cu-Co NSs resulted in the large electrode surface area to facilitate the glucose oxidation and a high sensitivity for glucose detection. As shown in Fig. 4A, the catalytic current density of Cu-Co NSs/RGO-CHIT/GCE was largest, indicating bimetallic nanomaterials exhibited better catalytic activities, which could be ascribed to the 3D dendritic Cu-Co NSs and synergetic effect. Sensitivity is a critical index to evaluate the performance of glucose sensor. The high sensitivity might be ascribed two aspects. On the one hand, the RGO improved the conductivity of Cu-Co NSs/CHIT-GO nanomaterials, which is helpful to electron transfer. On the other hand, the RGO-CHIT provided a large surface area to increase the quantity of Cu-Co NSs and also promoted the growth of 3D dendrites structure. In addition, the doping of Co atoms reduced the redox peaks potentials of $Cu(OH)_2$ and resulted in a low applied potential for glucose detection. The Co facilitated the Cu to reach a higher oxidation state during the oxidation process and accordingly promoted the electron transfer of glucose oxidation. The applied potential for electrocatalytic oxidation of glucose played a key role in improving the selectivity of sensor because the interference could be weaken at more negative potential.

4. Conclusions

A highly sensitive nonenzymatic glucose sensor was constructed based on the 3D dendritic nanocomposites electrodeposited on the RGO-CHIT/GCE by potentiostatic deposition method. The RGO-CHIT improved the conductivity of 3D dendritic Cu-Co NSs and the doping of Co resulted in 3D dendritic porous Cu-Co NSs with a large specific surface area, which enhanced the electron and mass transfer. The synergistic effect between Cu and Co resulted in a good catalytic activity and a low electrocatalytic oxidation potential for glucose. As a consequence, the as-prepared low-cost glucose sensor based on the 3D dendritic Cu-Co NSs/RGO-CHIT/GCE exhibited an excellent sensitivity, high stability, and good selectivity. It was successfully applied to the detection of glucose under coexistence of fetal calf serum. The results demonstrated good accuracy for the real samples. Overall, this work provides a simple method for the construction of nonenzymatic sensor for the rapid detection of glucose.

Acknowledgments

This work was financially supported by National Natural Science Foundation of China (21065005, 21165010 and 21101146), Young Scientist Foundation of Jiangxi Province (20112BCB23006 and 20122BCB23011) and the State Key Laboratory of Electroanalytical Chemistry (SKLEAC201310), Foundation of Jiangxi Educational Committee (GJJ13243 and GJJ13244), the Open Project Program of Key Laboratory of Functional Small organic molecule, Ministry of Education, Jiangxi Normal University (nos. KLFS-KF-201214; KLFS-KF-201218).

References

[1] Y.C. Zhang, L. Su, D. Manuzzi, H.V.E. de los Monteros, W.Z. Jia, D.Q. Huo, C.J. Hou, Y. Lei, Ultrasensitive and selective non-enzymatic glucose detection using copper nanowires, Biosensors and Bioelectronics 31 (2012) 426–432.
[2] J. Yang, L.C. Jiang, W.D. Zhang, S. Gunasekaran, A highly sensitive non-enzymatic glucose sensor based on a simple two-step electrodeposition of cupric oxide (CuO) nanoparticles onto multi-walled carbon nanotube arrays, Talanta 82 (2010) 25–33.
[3] L. Jin, L. Shang, S. Guo, Y. Fang, D. Wen, L. Wang, J. Yin, S. Dong, Biomolecule-stabilized Au nanoclusters as a fluorescence probe for sensitive detection of glucose, Biosensors and Bioelectronics 26 (2011) 1965–1969.
[4] O. Yehezkeli, R. Tel-Vered, S. Raichlin, I. Willner, Nano-engineered flavin-dependent glucose dehydrogenase/gold nanoparticle-modified electrodes for glucose sensing and biofuel cell applications, Acs Nano 5 (2011) 2385–2391.
[5] X. Du, I. Skachko, A. Barker, E.Y. Andrei, Approaching ballistic transport in suspended graphene, Nature Nanotechnology 3 (2008) 491–495.
[6] J.C. Meyer, A. Geim, M. Katsnelson, K. Novoselov, T. Booth, S. Roth, The structure of suspended graphene sheets, Nature 446 (2007) 60–63.
[7] F. Kim, L.J. Cote, J.X. Huang, Graphene oxide: surface activity and two-dimensional assembly, Advanced Materials 22 (2010) 1954–1958.
[8] G. Eda, M. Chhowalla, Chemically derived graphene oxide: towards large-area thin-film electronics and optoelectronics, Advanced Materials 22 (2010) 2392–2415.
[9] J. Ren, W. Shi, K. Li, Z. Ma, Ultrasensitive platinum nanocubes enhanced amperometric glucose biosensor based on chitosan and nafion film, Sensors and Actuators B: Chemical 163 (2012) 115–120.
[10] K. Khun, Z.H. Ibupoto, J. Lu, M.S. AlSalhi, M. Atif, A.A. Ansari, M. Willander, Potentiometric glucose sensor based on the glucose oxidase immobilized iron ferrite magnetic particle/chitosan composite modified gold coated glass electrode, Sensors and Actuators B: Chemical 173 (2012) 698–703.
[11] L. Masoomi, O. Sadeghi, M.H. Banitaba, A. Shahrjerdi, S.S.H. Davarani, A non-enzymatic nanomagnetic electro-immunosensor for determination of Aflatoxin B1 as a model antigen, Sensors and Actuators B: Chemical 177 (2013) 1122–1127.
[12] J.H. Shim, A. Cha, Y. Lee, C. Lee, Nonenzymatic amperometric glucose sensor based on nanoporous gold/ruthenium electrode, Electroanalysis 23 (2011) 2057–2062.
[13] J. Zeng, A simple eco-friendly solution phase reduction method for the synthesis of polyhedra platinum nanoparticles with high catalytic activity for methanol electrooxidation, Journal of Materials Chemistry 22 (2012) 3170–3176.
[14] L. Wei, Y.J. Fan, H.H. Wang, N. Tian, Z.Y. Zhou, S.G. Sun, Electrochemically shape-controlled synthesis in deep eutectic solvents of Pt nanoflowers with enhanced activity for ethanol oxidation, Electrochimica Acta 76 (2012) 468–474.
[15] A.P. Liu, Q.H. Ren, T. Xu, M. Yuan, W.H. Tang, Morphology-controllable gold nanostructures on phosphorus doped diamond-like carbon surfaces and their electrocatalysis for glucose oxidation, Sensors and Actuators B: Chemical 162 (2012) 135–142.
[16] Y. Huang, D.H. Kim, Light-controlled synthesis of gold nanoparticles using a rigid, photoresponsive surfactant, Nanoscale 4 (2012) 6312–6317.
[17] L. Wang, J.Y. Fu, H.Q. Hou, Y.H. Song, A facile strategy to prepare Cu_2O/Cu electrode as a sensitive enzyme-free glucose sensor, International Journal of Electrochemical Science 7 (2012) 12587–12600.
[18] J.W. Huang, Z.P. Dong, Y.D. Li, J. Li, J. Wang, H.D. Yang, S.W. Li, S.J. Guo, J. Jin, R. Li, High performance non-enzymatic glucose biosensor based on copper nanowires–carbon nanotubes hybrid for intracellular glucose study, Sensors and Actuators B: Chemical 182 (2013) 618–624.
[19] X.H. Kang, Z.B. Mai, X.Y. Zou, P.X. Cai, J.Y. Mo, A sensitive nonenzymatic glucose sensor in alkaline media with a copper nanocluster/multiwall carbon nano tube-modified glassy carbon electrode, Analytical Biochemistry 363 (2007) 143–150.
[20] C.W. Kung, C.Y. Lin, Y.H. Lai, R. Vittal, K.C. Ho, Cobalt oxide acicular nanorods with high sensitivity for the non-enzymatic detection of glucose, Biosensors & Bioelectronics 27 (2011) 125–131.
[21] J.Y. Zheng, Z.L. Quan, G. Song, C.W. Kim, H.G. Cha, T.W. Kim, W. Shin, K.J. Lee, M.H. Jung, Y.S. Kang, Vertical cobalt dendrite array films: electrochemical deposition and characterization, glucose oxidation and magnetic properties, Journal of Materials Chemistry 22 (2012) 12296–12304.
[22] Z.N. Liu, L.H. Huang, L.L. Zhang, H.Y. Ma, Y. Ding, Electrocatalytic oxidation of D-glucose at nanoporous Au and Au-Ag alloy electrodes in alkaline aqueous solutions, Electrochimica Acta 54 (2009) 7286–7293.
[23] D.Y. Liu, Q.M. Luo, F.Q. Zhou, Nonenzymatic glucose sensor based on gold-copper alloy nanoparticles on defect sites of carbon nanotubes by spontaneous reduction, Synthetic Metals 160 (2010) 1745–1748.
[24] S.S. Mahshid, S. Mahshid, A. Dolati, M. Ghorbani, L.X. Yang, S.L. Luo, Q.Y. Cai, Electrodeposition and electrocatalytic properties of Pt/Ni-Co nanowires for non-enzymatic glucose detection, Journal of Alloys and Compounds 554 (2013) 169–176.
[25] S.S. Mahshid, S. Mahshid, A. Dolati, M. Ghorbani, L. Yang, S. Luo, Q. Cai, Template-based electrodeposition of Pt/Ni nanowires and its catalytic activity towards glucose oxidation, Electrochimica Acta 58 (2011) 551–555.
[26] P. Yang, S.Y. Jin, Q.Z. Xu, S.H. Yu, Decorating PtCo bimetallic alloy nanoparticles on graphene as sensors for glucose detection by catalyzing luminol chemiluminescence, Small 9 (2013) 199–204.
[27] M. Jafarian, F. Forouzandeh, I. Danaee, F. Gobal, M.G. Mahjani, Electrocatalytic oxidation of glucose on Ni and NiCu alloy modified glassy carbon electrode, Journal of Solid State Electrochemistry 13 (2009) 1171–1179.
[28] C.L. Li, H.J. Wang, Y. Yamauchi, Electrochemical deposition of mesoporous Pt-Au alloy Films in aqueous surfactant solutions: towards a highly sensitive amperometric glucose sensor, Chemistry: A European Journal 19 (2013) 2242–2246.
[29] Y.P. Sun, H. Buck, T.E. Mallouk, Combinatorial discovery of alloy electrocatalysts for amperometric glucose sensors, Analytical chemistry 73 (2001) 1599–1604.

[30] J. Luo, S.S. Jiang, H.Y. Zhang, J.Q. Jiang, X.Y. Liu, A novel non-enzymatic glucose sensor based on Cu nanoparticle modified graphene sheets electrode, Analytica Chimica Acta 709 (2012) 47–53.
[31] Y.H. Song, Z.F. He, F.G. Xu, H.Q. Hou, L. Wang, pH-controlled electrocatalysis of amino acid based on electrospun cobalt nanoparticles-loaded carbon nanofibers, Sensors and Actuators B: Chemical 166–167 (2012) 357–364.
[32] M. Tabeshnia, M. Rashvandavei, R. Amini, F. Pashaee, Electrocatalytic oxidation of some amino acids on a cobalt hydroxide nanoparticles modified glassy carbon electrode, Journal of Electroanalytical Chemistry 647 (2010) 181–186.
[33] W.S. Hummers Jr., R.E. Offeman, Preparation of graphitic oxide, Journal of the American Chemical Society 80 (1958) 1339.
[34] D.X. Han, T.T. Han, C.S. Shan, A. Ivaska, L. Niu, Simultaneous determination of ascorbic acid, dopamine and uric acid with chitosan-graphene modified electrode, Electroanalysis 22 (2010) 2001–2008.
[35] A. Salimi, R. Hallaj, S. Soltanian, H. Mamkhezri, Nanomolar detection of hydrogen peroxide on glassy carbon electrode modified with electrodeposited cobalt oxide nanoparticles, Analytica Chimica Acta 594 (2007) 24–31.
[36] E. Gomez, A. Llorente, X. Alcobe, E. Valles, Electrodeposition for obtaining homogeneous or heterogeneous cobalt-copper films, Journal of Solid State Electrochemistry 8 (2004) 82–88.
[37] M. Jafarian, M.R. Avei, I. Danaee, F. Gobal, M.G. Mahjani, Electrochemical oxidation of saccharose on copper (hydr)oxide-modified electrode in alkaline media, Chinese Journal of Catalysis 31 (2010) 1351–1357.
[38] N. Torto, Recent progress in electrochemical oxidation of saccharides at gold and copper electrodes in alkaline solutions, Bioelectrochemistry 76 (2009) 195–200.
[39] X.C. Dong, H. Xu, X.W. Wang, Y.X. Huang, M.B. Chan-Park, H. Zhang, L.H. Wang, W. Huang, P. Chen, 3D Graphene–cobalt oxide electrode for high-performance supercapacitor and enzymeless glucose detection, ACS Nano 6 (2012) 3206–3213.
[40] Y. Ding, Y. Wang, L. Su, M. Bellagamba, H. Zhang, Y. Lei, Electrospun Co_3O_4 nanofibers for sensitive and selective glucose detection, Biosensors and Bioelectronics 26 (2010) 542–548.
[41] S. Priya, S. Berchmans, CuO microspheres modified glassy carbon electrodes as sensor materials and fuel cell catalysts, Journal of the Electrochemical Society 159 (2012) F73–F80.
[42] O. Karaagac, H. Kockar, M. Alper, M. Haciismailoglu, Influence of Co:Cu ratio on properties of Co-Cu films deposited at different conditions, Journal of Magnetism and Magnetic Materials 324 (2012) 3834–3838.
[43] Y. Yamauchi, T. Yokoshima, T. Momma, T. Osaka, K. Kuroda, Fabrication of magnetic mesostructured nickel-cobalt alloys from lyotropic liquid crystalline media by electroless deposition, Journal of Materials Chemistry 14 (2004) 2935–2940.
[44] Z.L. Xiao, C.Y. Han, W.K. Kwok, H.W. Wang, U. Welp, J. Wang, G.W. Crabtree, Tuning the architecture of mesostructures by electrodeposition, Journal of the American Chemical Society 126 (2004) 2316–2317.
[45] X.W. Wei, X.M. Zhou, K.L. Wu, Y. Chen, 3-D flower-like NiCo alloy nano/microstructures grown by a surfactant-assisted solvothermal process, Crystengcomm 13 (2011) 1328–1332.
[46] A.E. Mohamed, S.M. Rashwan, S.M. Abdel-Wahaab, M.M. Kamel, Electrodeposition of Co-Cu alloy coatings from glycinate baths, Journal of Applied Electrochemistry 33 (2003) 1085–1092.
[47] A.J. Bard, L.R. Faulkner, Electrochemical Methods, John Wiley and Sons, Inc., New York, 2001, pp. 156–225.
[48] A.J. Bard, L.R. Faulkner, Electrochemical Methods, John Wiley and Sons, Inc., New York, 2001, pp. 471–533.
[49] S.H. Zhou, X. Feng, H.Y. Shi, J. Chen, F. Zhang, W.B. Song, Direct growth of vertically aligned arrays of $Cu(OH)_2$ nanotubes for the electrochemical sensing of glucose, Sensors and Actuators B: Chemical 177 (2013) 445–452.
[50] P. Luo, S.V. Prabhu, R.P. Baldwin, Constant potential amperometric detection at a copper-based electrode: electrode formation and operation, Analytical Chemistry 62 (1990) 752–755.
[51] J. Yang, W.D. Zhang, S. Gunasekaran, An amperometric non-enzymatic glucose sensor by electrodepositing copper nanocubes onto vertically well-aligned multi-walled carbon nanotube arrays, Biosensors and Bioelectronics 26 (2010) 279–284.
[52] Z.J. Fan, B. Liu, X.H. Liu, Z.P. Li, H.G. Wang, S.G. Yang, J.Q. Wang, A flexible and disposable hybrid electrode based on Cu nanowires modified graphene transparent electrode for non-enzymatic glucose sensor, Electrochimica Acta 109 (2013) 602–608.
[53] J. Yang, W.D. Zhang, S. Gunasekaran, A low-potential H_2O_2-assisted electrodeposition of cobalt oxide/hydroxide nanostructures onto vertically-aligned multi-walled carbon nanotube arrays for glucose sensing, Electrochimica Acta 56 (2011) 5538–5544.
[54] L. Wang, X.P. Lu, Y.J. Ye, L.L. Sun, Y.H. Song, Nickel-cobalt nanostructures coated reduced graphene oxide nanocomposite electrode for nonenzymatic glucose biosensing, Electrochimica Acta 114 (2013) 484–493.
[55] C.X. Xu, F.L. Sun, H. Gao, J.P. Wang, Nanoporous platinum-cobalt alloy for electrochemical sensing for ethanol, hydrogen peroxide, and glucose, Analytica Chimica Acta 780 (2013) 20–27.
[56] X.L. Li, J.Y. Yao, F.L. Liu, H.C. He, M. Zhou, N. Mao, P. Xiao, Y.H. Zhang, Nickel/Copper nanoparticles modified TiO_2 nanotubes for non-enzymatic glucose biosensors, Sensors and Actuators B: Chemical 181 (2013) 501–508.

Biographies

Li Wang received her Ph.D. in analytical chemistry from the Changchun Institute of Applied Chemistry, Chinese Academy of Science, China. She is currently working as a professor at Jiangxi Normal University. Her current research interest is focused on electrochemical sensors.

Yaolin Zheng received his science bachelor in chemistry in 2012 from Jiangxi Normal University, China. He is working for his master's degree in Jiangxi Normal University, China. His research interests are nano-materials and their applications in sensor.

Xingping Lu received her science bachelor in chemistry in 2012 from Jiangxi Normal University, China. She is working for her master's degree in Jiangxi Normal University, China. Her research interests are nano-materials and their applications in sensor.

Zhuang Li is currently working as a professor at Changchun Institute of Applied Chemistry, Chinese Academy of Science, China. His current research interests focus on biosensors.

Lanlan Sun is currently working as an associate professor at State Key Laboratory of Luminescence and Applications, Changchun Institute of Optics, Fine Mechanics and Physics, Chinese Academy of Sciences. Her current research interests include nanostructured functional materials and their application for biosensors.

Yonghai Song received his Ph.D. in analytical chemistry from the Changchun Institute of Applied Chemistry, Chinese Academy of Science, China. He is currently working as a professor at Jiangxi Normal University. His current research interests focus on biosensors.